

Nuclear effects in the proton–deuteron Drell-Yan process

P. J. Ehlers^{1,2}, A. Accardi^{2,3}, L. T. Brady^{2,3*}, W. Melnitchouk²

¹*University of Minnesota – Morris, Morris, Minnesota 56267, USA*

²*Jefferson Lab, Newport News, Virginia 23606, USA*

³*Hampton University, Hampton, Virginia 23668, USA*

(Dated: July 9, 2014)

Abstract

We compute the nuclear corrections to the proton–deuteron Drell-Yan cross section for inclusive dilepton production, which, when combined with the proton–proton cross section, is used to determine the flavor asymmetry in the proton sea, $\bar{d} \neq \bar{u}$. In addition to nuclear smearing corrections that are known to be important at large values of the nucleon’s parton momentum fraction x_N , we also consider dynamical off-shell nucleon corrections associated with the modifications of the bound nucleon structure inside the deuteron, which we find to be significant at intermediate and large x_N values. We also provide estimates of the nuclear corrections at kinematics corresponding to existing and planned Drell-Yan experiments at Fermilab and J-PARC which aim to determine the \bar{d}/\bar{u} ratio for $x \lesssim 0.6$.

* Current address: University of California, Santa Barbara, California 93106, USA

I. INTRODUCTION

The discovery of the flavor asymmetry in the light quark sea in the proton, $\bar{d} \neq \bar{u}$, has been one of the most important findings in hadronic physics from the past two decades [1–6], stimulating considerable discussion about the nature and origin of the nucleon’s nonperturbative structure (see *e.g.* Refs. [7–10] for reviews). In particular, the Drell-Yan reaction, involving dilepton pair production in inclusive hadron–hadron scattering, has provided the most direct constraints on the x dependence of the \bar{d}/\bar{u} ratio [4–6]. Here, at the partonic level, a quark from the hadron beam annihilates with an antiquark from the target hadron (or vice versa), producing a high energy virtual photon which subsequently decays to a pair of oppositely charged leptons, $q\bar{q} \rightarrow \gamma^* \rightarrow \ell^+\ell^-$ [11]. By selecting specific values of the momentum fractions of the partons in the beam and target hadrons, one can construct ratios of cross sections with sensitivity to particular combinations of parton distribution functions (PDFs). In contrast to inclusive deep-inelastic lepton–nucleon scattering, which measures charge-even combinations of PDFs, $q + \bar{q}$, the Drell-Yan reaction has the advantage of allowing effects in the antiquark distributions to be cleanly isolated from those in the quark PDFs.

More specifically, the inclusive proton–free nucleon scattering cross section for the production of a lepton pair with invariant mass squared $Q^2 \gg M^2$, where M is the mass of the nucleon, is given (at leading order in the strong coupling) by

$$\sigma^{pN}(x_p, x_N) \equiv \frac{d\sigma^{pN}}{dx_p dx_N} = \frac{4\pi\alpha^2}{9Q^2} \sum_q e_q^2 \left[q(x_p)\bar{q}(x_N) + \bar{q}(x_p)q(x_N) \right], \quad (1)$$

where α is the fine-structure constant. In Eq. (1), $q(x_p)$ and $\bar{q}(x_N)$ are the quark and antiquark PDFs in the proton and target nucleon, evaluated at parton light-cone momentum fractions x_p and x_N of the proton and nucleon, respectively, e_q is the electric charge, and the sum is taken over all flavors q . (Here and throughout this paper, for ease of notation we omit the explicit Q^2 dependence in the arguments of PDFs and cross sections.) For the case of proton scattering from the deuteron, taking the ratio of pd to pp cross sections, and assuming the deuteron to be composed of a free proton and neutron, one can isolate the ratio of \bar{d} to \bar{u} distributions for large values of $x_p \gg x_N$ [12],

$$\frac{\sigma^{pd}}{\sigma^{pp}} \approx 1 + \frac{\bar{d}(x_N)}{\bar{u}(x_N)} \quad [x_p \gg x_N]. \quad (2)$$

The increase of the ratio $\sigma^{pd}/2\sigma^{pp}$ above unity observed at intermediate x values [4–6] has then been related directly to an excess of \bar{d} over \bar{u} in the proton.

Previous analyses of lepton-pair production in pd scattering have typically assumed that effects associated with the nuclear structure of the deuteron are negligible at the energies where the existing experiments [4–6] have been carried out. On the other hand, there has been a growing awareness of the need to account for nuclear corrections in precision determinations of PDFs, particularly at large values of x [13–16], where there is greatest sensitivity to the short-range structure of the nucleon–nucleon interaction. In deep-inelastic lepton scattering from the deuteron, for instance, nuclear smearing and nucleon off-shell effects have been included in a number of global PDF analyses [17–22], which have found significant effects on the d -quark distribution in particular at high x values ($x \gtrsim 0.5$). While the sea quark distributions in the proton do not extend to as large values of x as the valence quark distributions, the smearing effects become prominent at correspondingly smaller x values where the PDFs are falling most rapidly [23].

Recently Kamano and Lee [24] considered nuclear corrections to the pd Drell-Yan cross sections in a center of mass frame in which the projectile and target move with large longitudinal momentum. Boosting the deuteron wave function from the rest frame under the assumption that particle number is conserved, they found small corrections to the existing data from the Fermilab E866 experiment [5, 6], but potentially larger effects at $x \gtrsim 0.5$ for the new E906 (“SeaQuest”) experiment at lower energy [25]. Contributions from pion exchange between the proton and neutron in the deuteron were also found to be important at $x \gtrsim 0.4$ [24], which may appear surprising given that the small mass of the pion m_π is generally expected to restrict such effects to the region of $x \lesssim m_\pi/M \approx 0.15$. Earlier calculations of pion (and other meson) exchange effects in deep-inelastic lepton–deuteron scattering [26–28] showed a few percent overall enhancement (“antishadowing”) in the deuteron to nucleon structure function ratio at $x \sim 0.1$. An indirect feedback effect on quark distributions at large x could result from the conservation of valence quark number, although one might expect the major impact of the pion cloud to be on sea quark distributions.

In addition to Fermi motion and meson exchange effects, other corrections are also known to contribute to high energy nuclear cross sections, such as those associated with nuclear medium modification of the partonic structure of bound nucleons (nucleon off-shell corrections) [29–33], and final state interactions between the spectator nucleon in the deuteron

and the hadronic debris from the proton–nucleon collision [34]. While both of these corrections are difficult to constrain theoretically, their uncertainties are important to estimate for determining the overall errors on the PDF distributions, especially at large values of x .

In the present analysis we revisit the calculation of the proton–deuteron Drell-Yan cross section in Sec. II, paying particular attention to corrections associated with Fermi smearing and nucleon off-shell effects, which are expected to persist even at high energies. These corrections have received attention recently in several analyses [17–20] of deep-inelastic scattering from the deuteron, where their impact on PDFs and their uncertainties have been studied systematically in the context of global QCD fits using the “weak binding approximation” [13–15]. However, to date the global PDF analyses have not systematically included nuclear corrections to the pd Drell-Yan data, and it is important for a consistent determination of PDFs to consistently incorporate these in all data sets analyzed which involve deuterium nuclei.

In Sec. III we evaluate the pN cross section in terms of parton distributions in the bound nucleon. To take into account the possible modification of the nucleon structure due to interactions with the nuclear environment, we consider a relativistic spectator quark model in which the bound nucleon PDF is related to the change of the confinement radius of the nucleon in the deuteron. The approach is similar to the model developed in Refs. [14, 20], but in addition to valence quarks the model also includes the effects on sea quarks at small x . The combined effects of the nuclear smearing and off-shell corrections are illustrated in Sec. IV, where we discuss their impact on existing and planned Drell-Yan experiments at Fermilab [5, 6, 25] and J-PARC [35, 36]. Finally, in Sec. V we summarize our findings, and discuss their implications for future analyses of Drell-Yan cross sections and their constraints on parton distributions.

II. DRELL-YAN PROCESS IN PROTON–DEUTERON SCATTERING

In this section we present the derivation of the inclusive lepton pair production cross section for proton–deuteron scattering. After defining the relevant light-cone kinematics in the collinear frame, we describe how the pd cross section can be related to the corresponding nucleon-level cross section for proton scattering from bound nucleons in the deuteron.

A. Kinematics

We begin by defining the four-momenta of the virtual photon, beam proton, and target deuteron by q^μ , k^μ , and P_d^μ , respectively. To simplify the notation, we also introduce a rescaled deuteron momentum, $p_d^\mu \equiv (M/M_d)P_d^\mu$, where M_d is the deuteron mass, so that $p_d^2 = M^2$. In a frame of reference where the proton and deuteron are collinear (“ pd frame”) the momenta can be decomposed in terms of light-cone unit vectors \bar{n}^μ and n^μ ,

$$q^\mu = x_p k^+ \bar{n}^\mu + x_d p_d^- n^\mu + q_\perp^\mu, \quad (3a)$$

$$k^\mu = k^+ \bar{n}^\mu + \frac{M^2}{2k^+} n^\mu, \quad (3b)$$

$$p_d^\mu = \frac{M^2}{2p_d^-} \bar{n}^\mu + p_d^- n^\mu, \quad (3c)$$

where $\bar{n}^2 = n^2 = 0$ and $\bar{n} \cdot n = 1$, and the “plus” and “minus” light-cone components of any four-vector a are defined as $a^\pm = (a_0 \pm a_3)/\sqrt{2}$. The four-vector q_\perp^μ denotes the transverse momentum of the photon, with $q_\perp \cdot n = q_\perp \cdot \bar{n} = 0$, and $\mathbf{q}_\perp^2 = -q_\perp^\mu q_{\perp\mu}$ the square of the corresponding transverse three-momenta. The four-momentum of the nucleon in the deuteron is denoted by p^μ and can be similarly expanded as

$$p^\mu = \frac{p^2 + \mathbf{p}_\perp^2}{2zp_d^-} \bar{n}^\mu + zp_d^- n^\mu + p_\perp^\mu, \quad (4)$$

where the transverse momentum four-vector p_\perp^μ of the bound nucleon is defined such that $\mathbf{p}_\perp^2 = -p_\perp^\mu p_{\perp\mu}$. The variables x_p and x_d in Eq. (3a) are given by

$$x_p = \frac{q^+}{k^+}, \quad x_d = \frac{q^-}{p_d^-}, \quad (5)$$

and play the role of Nachtmann scaling variables for the Drell-Yan process, while the variable z in Eq. (4) represents the light-cone momentum fraction carried by the nucleon in the deuteron,

$$z = \frac{p^-}{p_d^-}. \quad (6)$$

Note that in the collinear frame, where the beam and target move in opposite directions, the proton and deuteron variables involve “plus” and “minus” components, respectively.

The experimentally measured (external) variables characterizing the process are the rescaled center of mass energy squared of the collisions, $s = (k + p_d)^2$, the dilepton invariant mass squared $Q^2 = (\ell + \bar{\ell})^2$, where ℓ and $\bar{\ell}$ are the four-momenta of the produced

lepton and antilepton. For convenience we also define the variable $\tilde{s} = 2k^+p_d^-$, in terms of which the center of mass energy squared can be written as $s = \tilde{s} + 2M^2 + M^4/\tilde{s}$, so that in the high energy limit, $\tilde{s} \gg M^2$, one has $s \rightarrow \tilde{s}$. From Eq. (3a) the photon virtuality can also be related to \tilde{s} as $Q^2 = x_p x_d \tilde{s} - \mathbf{q}_\perp^2$. In addition, one can define the dilepton rapidity y^* in the proton–deuteron center of mass frame (or “ pd frame”), in which $k^+ = p_d^-$,

$$y^* = \frac{1}{2} \log \frac{q^+}{q^-} \Big|_{k^+ = p_d^-}. \quad (7)$$

Note that, in contrast to the Lorentz invariants s and Q^2 , the rapidity generally depends on the frame of reference. The external variables are related to the Nachtmann light-cone momentum fractions by

$$x_p = \frac{Q_\perp}{\sqrt{\tilde{s}}} \exp(y^*), \quad x_d = \frac{Q_\perp}{\sqrt{\tilde{s}}} \exp(-y^*), \quad (8)$$

where $Q_\perp^2 = Q^2 + \mathbf{q}_\perp^2$ is the transverse mass of the dilepton, and inverting the relation between s and \tilde{s} , one has

$$\tilde{s} = \frac{s}{2} \left[1 - \frac{2M^2}{s} + \sqrt{1 - \frac{4M^2}{s}} \right]. \quad (9)$$

In the nuclear impulse approximation one assumes that the proton beam scatters incoherently from the individual proton or neutron in the deuteron. In relating the pd Drell-Yan cross section to the underlying proton–bound nucleon cross section, it will be convenient to introduce the (internal) nucleon level analog of the Nachtmann scaling variable,

$$x_N = \frac{q^-}{p^-} = \frac{x_d}{z}, \quad (10)$$

the pN center of mass energy squared,

$$s_N = (k + p)^2 = z\tilde{s} \left[1 + \frac{M^2 + p^2 + \mathbf{p}_\perp^2}{z\tilde{s}} + \frac{M^2(p^2 + \mathbf{p}_\perp^2)}{(z\tilde{s})^2} \right], \quad (11)$$

and the nucleon level rapidity,

$$y_N^* = \frac{1}{2} \log \frac{q^+}{q^-} \Big|_{k^+ = p^-} = y^* + \log \sqrt{z}, \quad (12)$$

where each of the variables has also been related to the external variables defined above. Note that the rapidity y_N^* here does not coincide with the rapidity of a free proton–bound nucleon collision, since the center of mass is slightly shifted by the transverse component of

the nucleon momentum [37]. While the kinematical relations in Eqs. (10)–(12) are exact, in practice the energies relevant for current and future Drell-Yan experiments are relatively large, with $s \gg M^2$. In the high energy limit, $s \rightarrow \infty$, one can therefore usually neglect hadron mass corrections and the transverse motion of the nucleon, in which case the proton and deuteron momentum fractions simplify to

$$x_p \approx \frac{Q_\perp}{\sqrt{s}} \exp(y^*), \quad x_d \approx \frac{Q_\perp}{\sqrt{s}} \exp(-y^*), \quad (13)$$

while the pN center of mass energy squared becomes $s_N \approx zs$. For the inclusive cross sections that will be considered here, with \mathbf{q}_\perp^2 integrated over, one can also assume $Q^2 \gg \mathbf{q}_\perp^2$, so that $Q_\perp \approx Q$.

B. Relation between deuteron and nucleon cross sections

The differential cross section for Drell-Yan lepton pair production in inclusive proton–deuteron scattering is defined as [37]

$$\frac{d\sigma^{pd}}{d^4q d\Omega} = \frac{1}{4\sqrt{(k \cdot p_d)^2 - M^4}} \frac{\alpha^2}{Q^4} L^{\mu\nu}(\ell, \bar{\ell}) W_{\mu\nu}^{pd}(k, p_d, q), \quad (14)$$

where Ω is the solid angle spanned by the lepton pair. The lepton tensor $L^{\mu\nu}$ is given by

$$L^{\mu\nu}(\ell, \bar{\ell}) = 2\ell^\mu \bar{\ell}^\nu + 2\ell^\nu \bar{\ell}^\mu - g^{\mu\nu}(\ell \cdot \bar{\ell} + m_\ell^2), \quad (15)$$

where m_ℓ is the lepton mass, which in our case is negligible. The proton–deuteron hadronic tensor (rescaled per-nucleon) is defined in terms of the matrix element of the commutator of the currents J_μ evaluated at the space-time points 0 and ζ ,

$$W_{\mu\nu}^{pd}(k, p_d, q) = \frac{M}{M_d} \int \frac{d^4\zeta}{(2\pi)^4} e^{iq \cdot \zeta} \langle k, p_d | [J_\mu(0), J_\nu(\zeta)] | k, p_d \rangle, \quad (16)$$

with the arguments defined in Sec. II A.

In the weak binding approximation, as is relevant for a weakly bound nucleus such as deuterium, the nucleon propagator in the nuclear medium can be expanded up to order \mathbf{p}^2/M^2 in the bound nucleon momentum [33, 38, 39]. This then allows the deuteron tensor to be factorized into a nucleon level tensor $\widetilde{W}_{\mu\nu}^{pN}$ and a deuteron spectral function ρ_d which describes the momentum distribution of the nucleons in the deuteron,

$$W_{\mu\nu}^{pd}(k, p_d, q) = \sum_N \int \frac{d^4p}{(2\pi)^4} \rho_d(p) \widetilde{W}_{\mu\nu}^{pN}(k, p, q), \quad (17)$$

where the sum is taken over the proton and neutron, $N = p + n$, and we assume charge symmetric nucleon distributions in the deuteron. A similar factorization can be obtained if one neglects antiparticle degrees of freedom, or treats the nucleons effectively as scalars [16]. In the impulse approximation, where the scattering takes place incoherently from individual nucleons in the nucleus, with the noninteracting “spectator” nucleon on its mass shell, the spectral function can be written in terms of the deuteron’s rest frame wave function ψ_d (which is a function of the nucleon’s three-momentum only),

$$\rho_d(\mathbf{p}) = \mathcal{N} (2\pi)^4 |\psi_d(\mathbf{p})|^2 \delta(p_0 + E_s - M_d), \quad (18)$$

where \mathcal{N} is a normalization factor, $E_s = \sqrt{M^2 + \mathbf{p}^2}$ is the spectator nucleon energy, and

$$p_0 = M_d - E_s \approx M + \varepsilon_d - \frac{\mathbf{p}^2}{2M} \quad (19)$$

is the energy of the interacting nucleon, with $\varepsilon_d = -2.2$ MeV the deuteron binding energy. In fact, the wave function depends on the magnitude of the nucleon’s three-momentum, $|\mathbf{p}|$, and is normalized such that $\int d^3\mathbf{p} |\psi_d(\mathbf{p})|^2 = 1$.

The specification of the deuteron rest frame in computing the spectral function in Eq. (18) breaks the relativistic covariance of the formalism, although typically Drell-Yan experiments are performed with the deuteron target at rest [5, 6, 25, 35]. Furthermore, the commonly used deuteron wave functions [40–42] are computed in the nonrelativistic approximation, and care must be taken to ensure that the correct normalization is preserved when reducing the full deuteron tensor, defined in terms of relativistic nucleon fields, to one expressed in terms of nonrelativistic wave functions. (Relativistic extensions of deuteron wave functions, which incorporate lower components of nucleon spinors, have also been used recently in high precision fits to NN scattering data [43].) Although the form of the normalization factor \mathcal{N} is not unique [30, 44], the choice $\mathcal{N} = M/p_0$ ensures conservation of the (Lorentz invariant) baryon number [33, 38], in contrast to the conservation of the (Lorentz non-invariant) particle number, discussed in Ref. [24]. With this choice, the differential pd cross section in Eq. (14) can be written in the deuteron rest frame as

$$\frac{d\sigma^{pd}}{dx_p dx_d d^2\mathbf{q}_\perp d\Omega} = \sum_N \int d^3\mathbf{p} \frac{M}{p_0} |\psi_d(\mathbf{p})|^2 \frac{\tilde{s}}{8M|\mathbf{p}|} \frac{\alpha^2}{Q^4} L^{\mu\nu} \widetilde{W}_{\mu\nu}^{pN}(k, p, q), \quad (20)$$

where we have used the relation $d^4q = k^+ p_d^- dx_p dx_d d^2\mathbf{q}_\perp$.

In analogy with Eq. (14), the product of the lepton tensor with the pN hadronic tensor in Eq. (20) is related to the proton-off-shell nucleon differential scattering cross section according to

$$\frac{d\tilde{\sigma}^{pN}}{dx_p dx_N d^2\mathbf{q}_\perp d\Omega} = \frac{z\tilde{s}}{8\sqrt{(k \cdot p)^2 - M^2 p^2}} \frac{\alpha^2}{Q^4} L^{\mu\nu} \widetilde{W}_{\mu,\nu}^{pN}(k, p, q), \quad (21)$$

where $dx_N = dx_d/z$. Integrating over the transverse photon momentum \mathbf{q}_\perp and $d\Omega$, the proton-deuteron cross section $\sigma^{pd}(x_p, x_d) \equiv d\sigma^{pd}/dx_p dx_d$ can therefore be written in terms of the pN cross section as

$$\sigma^{pd}(x_p, x_d) = \sum_N \int d^3\mathbf{p} |\psi_d(\mathbf{p})|^2 \frac{\sqrt{(k \cdot p)^2 - M^2 p^2}}{z p_0 |\mathbf{p}|} \tilde{\sigma}^{pN}\left(x_p, \frac{x_d}{z}, p^2\right), \quad (22)$$

where $\tilde{\sigma}^{pN} \equiv d\tilde{\sigma}^{pN}/dx_p dx_N$. Note that the proton-nucleon cross section here has an explicit dependence on p^2 , which reflects the possible modification of the nucleon structure due to interactions with other nucleons in the nucleus. This will require a generalization of the expression for the on-shell cross section in Eq. (1) to account for the dependence of the bound nucleon PDFs on p^2 , which in general does not vanish even in the high energy limit. For the case of the deuteron, where the spectator nucleon is on-mass-shell, the virtuality of the interacting nucleon p^2 can be related to \mathbf{p}_\perp^2 and z by $p^2 = -\mathbf{p}_\perp^2 M_d/(M_d - Mz) + p_{\text{max}}^2$, with $p_{\text{max}}^2 = zM(M_d^2 - M^2 - zMM_d)/(M_d - Mz)$. The off-shell generalization of the pN cross section and the parton distributions in the bound nucleon will be discussed in Sec. III B.

C. Convolution and nuclear smearing function

In practical applications of the cross section relation in Eq. (22) it is convenient to express the three-dimensional integration over \mathbf{p} in terms of integrations over the light-cone fraction z and the transverse momentum p_\perp^2 , as defined in Sec. II A,

$$\int d^3\mathbf{p} = \int dz d\mathbf{p}_\perp^2 \frac{\pi M E_s}{M_d - Mz}, \quad (23)$$

where the integration over the azimuthal angle has been performed. The on-shell spectator condition restricts the nucleon momentum to be $\mathbf{p}^2 = \mathbf{p}_\perp^2 + p_z^2$, where the longitudinal momentum is given by $p_z = [\mathbf{p}_\perp^2 + M^2 - (M_d - Mz)^2]/2(M_d - Mz)$. Using these relations, the pd cross section can then be written as

$$\sigma^{pd}(x_p, x_d) = \sum_N \int \frac{dz}{z} d\mathbf{p}_\perp^2 f(z, \mathbf{p}_\perp^2) \tilde{\sigma}^{pN}\left(x_p, \frac{x_d}{z}, p^2\right), \quad (24)$$

where

$$f(z, \mathbf{p}_\perp^2) = \frac{\pi M E_s}{M_d - Mz} \frac{\sqrt{(k_0 p_0 + |k_z| p_z)^2 - M^2 p^2}}{|k_z| p_0} |\psi_d(\mathbf{p})|^2 \quad (25)$$

is the z - and \mathbf{p}_\perp -dependent light-cone momentum distribution of nucleons in the deuteron (or unintegrated smearing function). In the high energy limit, as is considered in the applications here, where $k_0^2 \gg p^2 + \mathbf{p}_\perp^2 \lesssim \mathcal{O}(1 \text{ GeV}^2)$, one can approximate the function $f(z, \mathbf{p}_\perp^2)$ by

$$f(z, \mathbf{p}_\perp^2) \approx \frac{\pi M E_s}{M_d - Mz} \left(1 + \frac{p_z}{p_0}\right) |\psi_d(\mathbf{p})|^2. \quad (26)$$

This result coincides with the smearing function for deep-inelastic scattering computed in the Bjorken limit [14, 16], and is automatically normalized to unity. A simplified convolution in terms of one-dimensional smearing functions can be obtained if the off-shell nucleon cross section is expanded around its on-shell limit, $p^2 = M^2$,

$$\tilde{\sigma}^{pN}(x_p, x_N, p^2) \approx \sigma^{pN}(x_p, x_N) \left[1 + \frac{(p^2 - M^2)}{M^2} \delta\sigma^{pN}(x_p, x_N)\right], \quad (27)$$

where $\sigma^{pN}(x_p, x_N) \equiv \tilde{\sigma}^{pN}(x_p, x_N, M^2)$ is the on-shell proton–nucleon cross section, and

$$\delta\sigma^{pN}(x_p, x_N) = \left. \frac{\partial \log \tilde{\sigma}^{pN}}{\partial \log p^2} \right|_{p^2=M^2} \quad (28)$$

is the lowest order off-shell correction. Higher order terms in this expansion are suppressed by additional powers of $(p^2 - M^2)/M^2 \approx 2(\varepsilon_d - \mathbf{p}^2/M)/M$. The expansion (27) then enables the \mathbf{p}_\perp dependence of the integrand to be factorized into a \mathbf{p}_\perp -integrated (on-shell) smearing function $f(z)$ and an off-shell smearing function $f^{(\text{off})}(z)$,

$$\sigma^{pd}(x_p, x_d) = \sum_N \int_{x_d}^1 \frac{dz}{z} \left[f(z) + f^{(\text{off})}(z) \delta\sigma^{pN}\left(x_p, \frac{x_d}{z}\right) \right] \sigma^{pN}\left(x_p, \frac{x_d}{z}\right), \quad (29)$$

where

$$f(z) = \int d\mathbf{p}_\perp^2 f(z, \mathbf{p}_\perp^2), \quad (30)$$

and

$$f^{(\text{off})}(z) = \int d\mathbf{p}_\perp^2 \frac{p^2 - M^2}{M^2} f(z, \mathbf{p}_\perp^2). \quad (31)$$

The result (29) is analogous to the generalized convolution expressions for deep-inelastic nuclear structure functions [14] in the high energy limit, corresponding in particular to the F_1^d structure function rather than F_2^d (or $x F_1^d$).

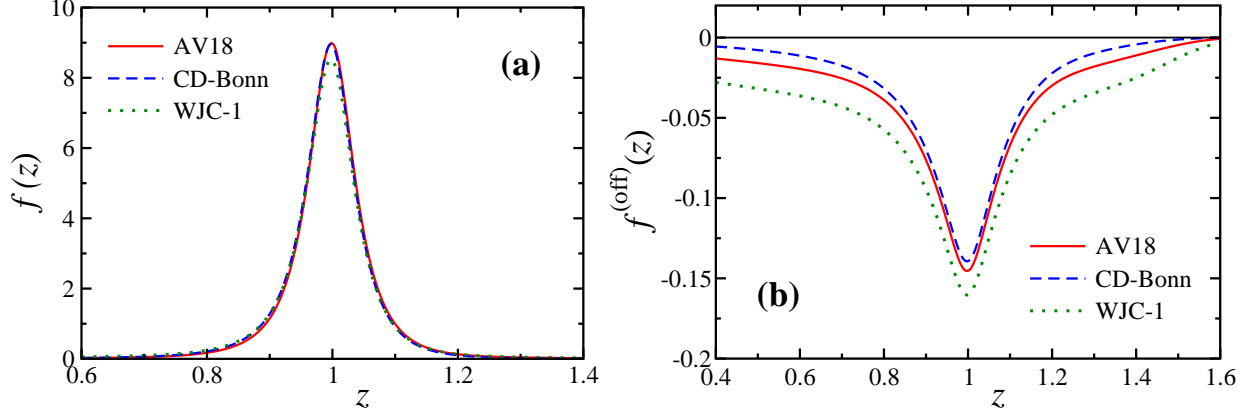


FIG. 1: Nucleon smearing functions in the deuteron: **(a)** on-shell distribution $f(z)$ and **(b)** off-shell function $f^{\text{off}}(z)$, for the AV18 [41] (solid lines), CD-Bonn [42] (dashed lines), and WJC-1 [43] (dotted lines) deuteron wave functions.

The z dependence of the smearing function $f(z)$ and the off-shell correction $f^{(\text{off})}(z)$ is illustrated in Fig. 1, for several deuteron wave functions, based on the AV18 [41], CD-Bonn [42] and WJC-1 [43] nucleon–nucleon potentials. As expected, the on-shell function $f(z)$ peaks strongly around $z \approx 1$, and falls off rapidly away from the peak. The wave function dependence is relatively weak, except at large $|z - 1|$ [45]. Since the WJC-1 wave function has the hardest momentum distribution of the models considered, the magnitude of the smearing function is correspondingly smaller at the peak in order to preserve the correct normalization. In contrast, the off-shell smearing function $f^{(\text{off})}(z)$ displays a relatively stronger dependence on the deuteron wave function, with the largest magnitude for the WJC-1 model and smallest magnitude for the CD-Bonn wave function. The negative sign of $f^{(\text{off})}(z)$ arises from the $p^2 - M^2$ factor in the integrand in Eq. (31), since the virtuality of the off-shell nucleon is always less than M^2 . The small values of the deuteron binding energy and average three-momentum distribution suppress the magnitude of the off-shell function relative to $f(z)$ by about an order of magnitude. However, as we shall see in the next section, where we discuss the calculation of the pN cross section at the partonic level, the off-shell corrections can have a significant effect on the overall pd cross section.

III. PARTON LEVEL CROSS SECTION

To compute the pd cross section in Eq. (29) requires calculation of the nucleon-level cross section in terms of PDFs of the beam proton and bound nucleon in the target deuteron. In this section we derive the proton-bound nucleon cross section, working to leading order accuracy in the strong coupling. After defining the kinematics relevant for the parton-level process, we express the off-shell pN cross section in terms of off-shell generalizations of PDFs in the bound nucleon, and construct a simple model to describe the possible p^2 dependence of the off-shell PDFs.

A. Parton-parton scattering

In analogy with the definition of the external momentum variables in the pd frame in Eqs. (3), we decompose the four-momenta of the colliding partons in the proton (\hat{k}) and nucleon (\hat{p}) in terms of the light-cone vectors n^μ and \bar{n}^μ ,

$$\hat{k}^\mu = \hat{k}^+ \bar{n}^\mu + \frac{\hat{k}^2 + \hat{\mathbf{k}}_\perp^2}{2\hat{k}^+} n^\mu + \hat{k}_\perp^\mu, \quad (32a)$$

$$\hat{p}^\mu = \frac{\hat{p}^2 + \hat{\mathbf{p}}_\perp^2}{2\hat{p}^-} \bar{n}^\mu + \hat{p}^- n^\mu + \hat{p}_\perp^\mu, \quad (32b)$$

where \hat{k}^2 and \hat{p}^2 are the partons' virtualities and \hat{k}_\perp^μ and \hat{p}_\perp^μ the respective transverse momentum four-vectors. In the collinear factorization framework, the total pN amplitude at leading twist is expressed as a product of the partonic hard scattering amplitude and the soft, nonperturbative parton distributions in the hadrons. The partonic amplitude is calculated by expanding the parton momentum about the direction of motion of the parent hadron and about the parton's on-shell limit [46–48]. The hard scattering process can thus be computed by setting the partonic momenta in Eqs. (32) to

$$\hat{k}^+ \rightarrow \xi_p k^+, \quad \hat{k}_\perp^\mu \rightarrow 0, \quad (33a)$$

$$\hat{p}^- \rightarrow \xi_N p^-, \quad \hat{p}_\perp^\mu \rightarrow \xi_N p_\perp^\mu, \quad (33b)$$

which defines the partonic light-cone momentum fractions ξ_p and ξ_N in the proton and target nucleon, respectively. For light quarks, without loss of generality, one can take the (on-shell) quarks to be massless, so that

$$\hat{k}^2 \rightarrow 0, \quad \hat{p}^2 \rightarrow 0. \quad (34)$$

At leading order in the strong coupling, the quark–antiquark pair fuses into a virtual photon, which subsequently decays into a dilepton. Conservation of four-momentum, $q^\mu = \hat{k}^\mu + \hat{p}^\mu$, then implies that the momentum fractions are related by

$$\xi_N = x_N = \frac{x_d}{z}, \quad \xi_p = \frac{Q^2}{Q_\perp^2} x_p, \quad (35)$$

which can be obtained by equating the “−” and “+” components, respectively, while from the transverse components one has $\mathbf{q}_\perp^2 = x_N^2 \mathbf{p}_\perp^2$. Since the average transverse momentum of the bound nucleon is $\langle \mathbf{p}_\perp^2 \rangle \approx p_F^2 \sim 0.1 \text{ GeV}^2$, with p_F the deuteron Fermi momentum, one can therefore neglect the transverse momentum compared to the dilepton mass Q^2 . At high energies one then obtains $\xi_p \approx x_p$. In this limit the proton–off-shell nucleon cross section becomes

$$\tilde{\sigma}^{pN}(x_p, x_N, p^2) = \frac{4\pi\alpha^2}{9x_p x_N s_N} \sum_q e_q^2 [q(x_p) \tilde{q}(x_N, p^2) + \bar{q}(x_p) \tilde{q}(x_N, p^2)], \quad (36)$$

where $\tilde{q}(x_N, p^2)$ is the PDF for a quark in an off-shell nucleon with virtuality p^2 , such that in the on-shell limit, $p^2 \rightarrow M^2$, one has $\tilde{q}(x_N, M^2) \equiv q(x_N)$. Note that at high energy $x_N s_N \approx x_d s$, so that the dependence on z enters only through the PDF arguments, and the entire off-shell dependence of the cross section is contained in the p^2 dependence of the PDFs. In the next section we estimate this dependence in a simple spectator model of the nucleon.

B. Off-shell corrections

In the absence of a first principles calculation of the nuclear bound state in terms of quark and gluons degrees of freedom, computing the off-shell behavior of PDFs is rather challenging. Several attempts have been made in the literature to estimate the p^2 dependence of the off-shell distribution \tilde{q} within effective quark models [14, 29, 32, 49]. Generally the models give rise to a suppression of the PDFs as a function of x , although the quantitative features of the off-shell modification depend somewhat on the details of the specific model.

In this analysis we adopt the “modified Kulagin-Petti” model [14] for the valence distributions, used recently in the CJ global PDF analyses [19, 20] which focused on the high- x region, and extend it to the sea quark sector to describe the off-shell PDFs at both small and large x . An attractive feature of this model is that the corrections can be related to

the average virtuality of the bound nucleons in the nuclear medium, and the corresponding change of the nucleon's confinement radius. The valence PDFs for the bound nucleons are further constrained by baryon number conservation, so that the off-shell corrections do not alter the normalization.

In analogy with Eq. (27), we expand the off-shell PDF $\tilde{q}(x, p^2)$ to lowest order about its on-shell mass limit,

$$\tilde{q}(x, p^2) = q(x) \left[1 + \frac{(p^2 - M^2)}{M^2} \delta q(x) \right], \quad (37)$$

where the off-shell correction $\delta q(x)$ is given by

$$\delta q(x) = \frac{\partial \log \tilde{q}}{\partial \log p^2} \Big|_{p^2=M^2}. \quad (38)$$

Using Eqs. (21), (27) and (37), the off-shell correction to the proton–nucleon Drell–Yan cross section can be written as

$$\sigma^{pN} \delta \sigma^{pN} = \frac{4\pi\alpha^2}{9x_p x_N s_N} \sum_q e_q^2 [q(x_p) \bar{q}(x_N) \delta \bar{q}(x_N) + \bar{q}(x_p) q(x_N) \delta q(x_N)], \quad (39)$$

where the $(p^2 - M^2)$ term in Eq. (27) has been factored out. At the parton level, the pd differential cross section can then be expressed (at leading order) in terms of the PDFs in the beam proton and target deuteron,

$$\sigma^{pd}(x_p, x_d) = \frac{4\pi\alpha^2}{9x_p x_d s_N} \sum_q e_q^2 [q(x_p) \bar{q}^d(x_d) + \bar{q}(x_p) q^d(x_d)], \quad (40)$$

where, in analogy with Eq. (29), the PDF in the deuteron, q^d , is given by

$$q^d(x_d) = \sum_N \int_{x_d}^1 \frac{dz}{z} \left[f(z) + f^{(\text{off})}(z) \delta q\left(\frac{x_d}{z}\right) \right] q^N\left(\frac{x_d}{z}\right), \quad (41)$$

which includes corrections from nuclear smearing and nucleon off-shell effects.

To evaluate the off-shell correction one assumes that the p^2 -dependent PDF can be represented in terms of a spectral function D_q [14, 33],

$$\tilde{q}(x, p^2) = \int dw^2 \int_{-\infty}^{\hat{p}_{\text{max}}^2} d\hat{p}^2 D_q(w^2, \hat{p}^2, x, p^2), \quad (42)$$

where $w^2 = (p - \hat{p})^2$ is the mass of the (on-shell) spectator quarks in the bound nucleon, and \hat{p}^2 is the interacting quark's virtuality, with a maximum value $\hat{p}_{\text{max}}^2 = x [p^2 - w^2 / (1 - x)]$. Note that since the PDF in Eq. (42) represents the soft, nonperturbative parton momentum

distribution in the nucleon, there is no hard scale to suppress contributions from off-shell partons, in contrast to the hard scattering kinematics in Eqs. (33a). However, the spectral function D_q must fall off sufficiently fast at large \hat{p}^2 so as to ensure convergence of the spectral integral.

Following Refs. [14, 19, 33, 38], we use the single-pole approximation in which the spectator spectrum is represented by a single (on-shell) state with effective mass \bar{w}_q^2 for a given quark flavor q ,

$$D_q = \delta(w^2 - \bar{w}_q^2) \Phi_q(\hat{p}^2, \Lambda(p^2)). \quad (43)$$

Here the function Φ_q describes the momentum distribution of quarks with virtuality \hat{p}^2 in the off-shell nucleon, and the scale parameter $\Lambda(p^2)$ suppresses contributions from large \hat{p}^2 . Note that in this approximation the x dependence of the off-shell distribution \tilde{q} arises from the upper limit on the \hat{p}^2 integration in Eq. (42), which depends on x as well as on w^2 and p^2 . In Ref. [14] the scale Λ was related to the confinement radius R_N of the nucleon, $\Lambda \sim 1/R_N$, which allows the p^2 dependence of Λ to be interpreted in terms of the change in the nucleon radius when the nucleon is bound inside the deuteron. Using Eq. (43), the off-shell correction δq in Eq. (37) can then be written

$$\delta q(x) = C_q + \frac{\partial \log q}{\partial x} h_q(x), \quad (44)$$

where C_q is determined by PDF normalization constraints, and

$$h_q(x) = x(1-x) \frac{(1-\lambda)(1-x) + \lambda \bar{w}_q^2/M^2}{(1-x)^2 - \bar{w}_q^2/M^2}, \quad (45)$$

with the parameter λ defined as

$$\lambda = \left. \frac{\partial \log \Lambda^2}{\partial \log p^2} \right|_{p^2=M^2}. \quad (46)$$

Since the cutoff Λ is inversely proportional to R_N , one can also write the λ parameter as $\lambda = -2(\delta R_N/R_N)(\delta p^2/M^2)$, where δR_N is the change in the nucleon's radius in the nuclear medium, and $\delta p^2/M^2 = \int dz f^{(\text{off})}(z)$ is the average nucleon virtuality in the deuteron. The value of δp^2 depends on the NN potential model, and ranges between $\delta p^2/M^2 \approx -3.6\%$ and -6.5% for the CD-Bonn [42] and WJC-1 [43] deuteron wave functions, respectively, with other wave functions such as Paris [40] and AV18 [41] giving intermediate values. Estimates of the change in confinement radius in the deuteron based on the analysis of data on the

nuclear EMC effect suggest [50] a value for $\delta R_N/R_N \sim \mathcal{O}(1\% - 2\%)$. In Ref. [20] the uncertainties in the off-shell corrections were estimated by considering several combinations of the deuteron wave function and the nucleon “swelling”, and were represented in the form of the “CJ12min” (small nuclear correction), “CJ12mid” (medium nuclear correction) and “CJ12max” (large correction) PDFs. These correspond, respectively, to the WJC-1 wave function (hardest) with a 0.3% nucleon swelling, the AV18 wave function with a 1.2% swelling effect, and the CD-Bonn wave function (softest) with a 2.1% nucleon swelling.

In previous calculations of off-shell corrections to PDFs using this type of model [14, 19, 33, 38] (which, following Ref. [51], we refer to generally as the “off-shell covariant spectator” or OCS model), only valence quark distributions were studied. However, with reasonable approximations it is straightforward to extend this model to compute the off-shell corrections to sea quark (and gluon) distributions, as needed in the analysis of Drell-Yan data. (We include gluons here for completeness, even though the gluon PDF does not enter explicitly in the leading order Drell-Yan cross section; it will be relevant, however, for next-to-leading order calculations.) The essential difference will be in the values of the spectator effective mass \overline{w}_q^2 for a given parton flavor. Within the OCS model framework, a fit to existing PDFs in the free proton gives $\overline{w}_v^2 = 2.2 \text{ GeV}^2$, $\overline{w}_s^2 = 5.5 \text{ GeV}^2$, and $\overline{w}_g^2 = 8.0 \text{ GeV}^2$ for the valence, sea, and gluon distributions, respectively. The valence mass parameter is similar to that found in Ref. [14], and the larger masses for the sea quark and gluon distributions reflect the larger minimum number of partons required in the intermediate state for sea quarks and gluons compared to valence quarks.

The normalization constant C_q in Eq. (44) is computed for valence quarks $q_v = q - \bar{q}$ by requiring that the off-shell correction does not alter the baryon number [19],

$$\int_0^1 dx q_v(x) \delta q_v(x) = 0. \quad (47)$$

For sea quarks and gluons, on the other hand, perturbative radiation of soft gluons and generation of $q\bar{q}$ pairs render the corresponding integrals infinite. To proceed one can either impose a constraint from a higher moment, such as the momentum sum rule, or alternatively consider a model of the nucleon at a low momentum scale involving a finite number of partonic degrees of freedom. Parametrizations based on this boundary condition have long been utilized by the Dortmund group [52–54], for example, assuming valence-like gluon and sea PDFs at low Q^2 , and generating the high- Q^2 dependence through perturbative evolution.

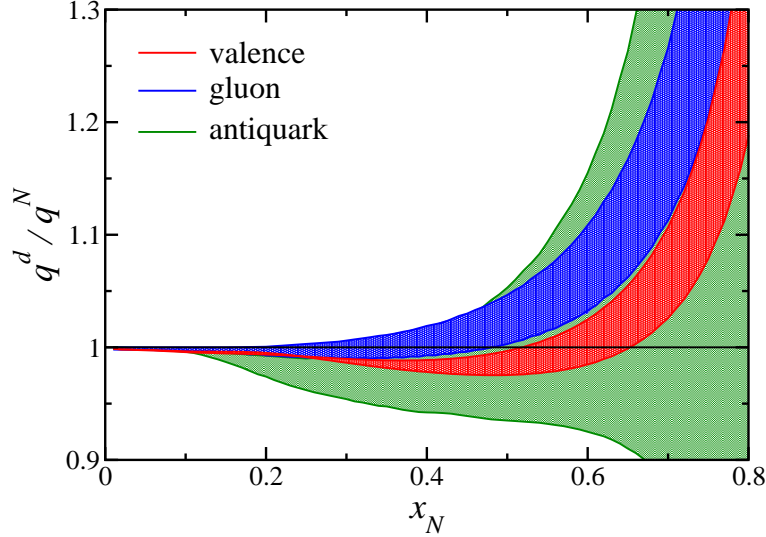


FIG. 2: Ratio of PDFs in the deuteron to those in an isoscalar nucleon, q^d/q^N , for valence $q = u_v + d_v$ quarks (red shaded band), antiquarks $q = \bar{u} + \bar{d}$ (green shaded band), and gluons (blue shaded band), including the effects of nuclear smearing and nucleon off-shell corrections. The bands represent the range of deuteron wave functions and nucleon off-shell parameters used in Ref. [20].

This in fact is closer in spirit to the spectral function model of Eq. (42) with finite values of the spectator system mass \bar{w}_q^2 .

We considered both methods of determining the sea normalization, but found relatively small differences at medium to high values of x ($x \gtrsim 0.3$). At smaller x , results from Drell-Yan measurements of cross section ratios of C, Ca, Fe and W to deuterium [55, 56] in the Fermilab E772 experiment disfavor large medium modifications of antiquark distributions for $0.1 \lesssim x \lesssim 0.3$. In this range, the OCS model with the momentum sum rule constraint gives a fairly small correction, albeit with sizeable uncertainty, and to ensure consistency with the E772 Drell-Yan data we therefore smoothly extrapolate the corrections to zero below $x \approx 0.15$.

The ratios q^d/q^N of the PDFs in the deuteron, calculated through Eq. (41), to those in an isoscalar nucleon ($N = p + n$) are illustrated in Fig. 2 for the valence quark $u_v + d_v$, sea quark (or antiquark) $\bar{u} + \bar{d}$, and gluon distributions. For consistency with the original analysis of the Drell-Yan data from the E866 experiment [6], we use the input nucleon PDFs from the CTEQ5 global QCD analysis [57] as in Ref. [6]. The distributions in the deuteron include the effects of nuclear smearing and nucleon off-shell corrections, with the bands in

Fig. 2 illustrating the maximal range from different models of the deuteron wave function and nucleon “swelling” parameters, as discussed above. Specifically, the upper edges of the bands, with the largest q^d/q^N ratios, correspond to the smallest nuclear corrections (WJC-1 deuteron wave function with a 0.3% nucleon swelling), while the lower edges correspond to stronger nuclear corrections (CD-Bonn wave function and up to $\sim 2\%$ nucleon swelling).

The effects of the nuclear smearing are evident in the rise above unity at $x \gtrsim 0.5$ of the valence quarks and gluon ratios, characteristic of nuclear deep-inelastic structure function ratios in the nuclear EMC effect [20]. The behavior of the antiquark ratios for the smallest nuclear corrections is similar at intermediate and large x , while for the strongest nuclear corrections the ratio stays below unity over the range $x \lesssim 0.7$ over which the antiquark PDFs are determined in the CTEQ5 fit [57]. The large spread in the antiquark ratios for $x \gtrsim 0.4$ results from a combined effect of the nuclear correction uncertainties, and the very small size (with large uncertainty) of the \bar{u} and \bar{d} PDFs in this region.

Finally, we also note that the general form of the convolution in Eqs. (40) and (41) closely resembles the result obtained recently by Kamano and Lee [24], although with some important differences. In particular, whereas the momentum fraction z here is defined in the context of collinear factorization on the light-cone [58], as a fraction of the “minus” components of the proton and deuteron four-vectors [Eq. (6)], in Ref. [24] it is related to the ratio p_z/p_z^{ave} of the nucleon’s longitudinal momentum relative to its quadratic average with respect to the deuteron wave function, $p_z^{\text{ave}} = \langle p_z^2 \rangle^{1/2}$. Therefore, although the formal expressions for the pd cross sections are similar, a direct comparison of the cross sections derived here and in Ref. [24] is difficult because of the different frames and variables used in the two approaches. An advantage of the present approach is that by working with light-cone momentum fractions our results are invariant under Lorentz boosts along the light-front. In practice we perform the calculation in the rest frame of the deuteron, so that no approximations need to be made in boosting the deuteron wave function.

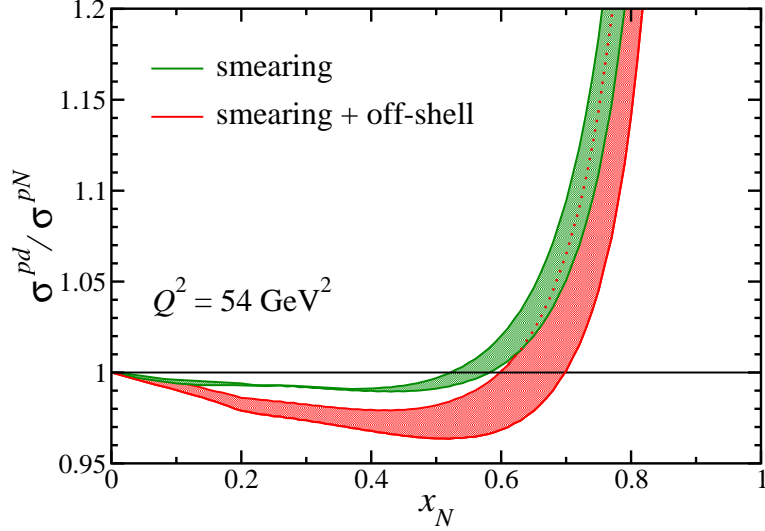


FIG. 3: Ratio of pd to pN Drell-Yan cross sections σ^{pd}/σ^{pN} at the kinematics corresponding to the Fermilab E866 experiment [6] (incident proton energy $k_0 = 800$ GeV and average $Q^2 = 54$ GeV 2), including the effects of nuclear smearing (green band) and smearing + nucleon off-shell corrections. The band for the smearing only corrections represents the range defined by the WJC-1 [43], AV18 [41] and CD-Bonn [42] deuteron wave functions, while the smearing + off-shell band includes in addition the range of nucleon off-shell (swelling) parameters [20].

IV. NUCLEAR EFFECTS ON CROSS SECTION RATIOS

Using the formalism for the pd Drell-Yan cross section derived in Sec. II and the OCS model for the off-shell nucleon PDFs in the deuteron in Sec. III, we can proceed to compute the nuclear effects in the pd dilepton production reaction by comparing them with the corresponding proton-free nucleon scattering process. In Fig. 3 we illustrate the effects of the nuclear corrections in the ratio of the pd to the isoscalar nucleon pN Drell-Yan cross section, computed at the kinematics of the Fermilab E866 [6] experiment (incident energy $k_0 = 800$ GeV and average $Q^2 = 54$ GeV 2). The ratio displays the characteristic shape of the nuclear EMC effect, with a small, few percent depletion at intermediate values of x ($x \lesssim 0.5$) and a rapid rise above unity at larger x ($x \gtrsim 0.6$). The greater spread in the calculated ratio in the high- x region ($x \gtrsim 0.5$) reflects the larger uncertainties in the deuteron wave function at short distances, or large z in the nuclear smearing function in Fig. 1. The nucleon off-shell corrections act to reduce the pd cross section over most of the range of x , resulting in a more sizeable nuclear effect at intermediate x ($0.2 \lesssim 0.6$). The overall uncertainty also increases

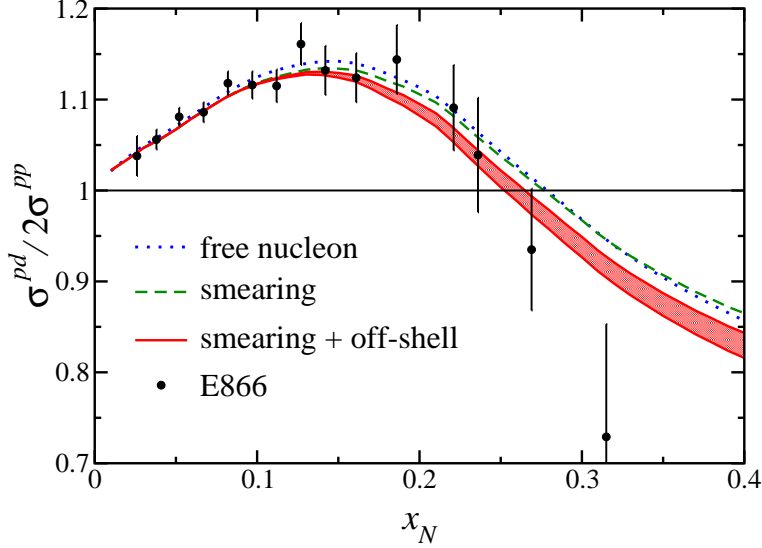


FIG. 4: Ratio of pd to pp Drell-Yan cross sections $\sigma^{pd}/2\sigma^{pp}$ at the kinematics of the Fermilab E866 data [6], with incident proton energy $k_0 = 800$ GeV and average $Q^2 = 54$ GeV². The E866 data (filled circles) are compared with the free nucleon calculation without any nuclear effects (blue dotted curve), with nuclear smearing corrections only (green dashed curve), and with nuclear smearing + off-shell corrections (red solid band).

due to the range of possible behaviors of the bound nucleon PDFs, as discussed in Sec. III.

The reduction of the pd Drell-Yan cross section in the presence of nuclear corrections, relative to the pN cross section, is clearly visible in the pd to pp cross section ratio shown in Fig. 4. While the effect of the nuclear smearing is relatively mild over the range of x covered by the Fermilab E866 data, $0.02 \lesssim x \lesssim 0.3$ (qualitatively similar to that found in Ref. [24]), the addition of nucleon off-shell corrections lowers the overall free-nucleon cross section appreciably for $x \gtrsim 0.1 - 0.2$. An intriguing feature of the E866 data is the apparent reduction of the pd to pp cross section ratio below unity at the two largest- x data points, albeit with large uncertainties, suggesting a possible sign change of $\bar{d} - \bar{u}$ for $x \gtrsim 0.25$. By lowering the pd cross sections in this region, the nuclear corrections computed here improve the agreement with the data in this region (using the CTEQ5 PDF set [57]), although it is unlikely that this can account for the entire effect at large x .

To better understand the large- x behavior of \bar{d}/\bar{u} , the new Fermilab SeaQuest experiment (“SeaQuest”), using a lower proton beam energy of $k_0 = 120$ GeV, was proposed to measure the pd to pp Drell-Yan cross section ratio to $x \approx 0.45$ [25]. With the expected precision

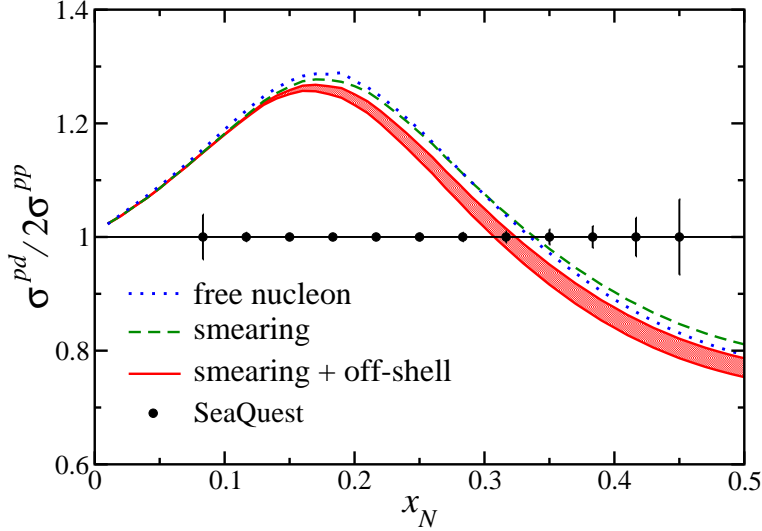


FIG. 5: Ratio of pd to pp Drell-Yan cross sections as in Fig. 4, but at the kinematics of the new Fermilab SeaQuest experiment [25], with incident proton energy $k_0 = 120$ GeV and average $Q^2 = 42$ GeV². The projected data (filled circles) with estimated uncertainties are arbitrarily placed at unity.

of the data illustrated in Fig. 5, this measurement should unambiguously determine the trend of the \bar{d}/\bar{u} ratio in the $x \approx 0.3 - 0.4$ region. Computing the nuclear effects on the pd cross section at the SeaQuest kinematics, the impact of the nuclear smearing and off-shell corrections is comparable to or even larger than the projected uncertainties for $0.15 \lesssim x \lesssim 0.4$. This suggests that the overall systematic uncertainties in the measurement may be underestimated in this region, and that further work may be needed in order to better constrain the theoretical uncertainties in the calculation of the nuclear corrections to the pd cross section. The SeaQuest experiment commenced data taking in 2014, and is expected to run until late 2015, with first results anticipated by the end of 2014 [59].

Beyond the Fermilab experiments, a proposal has been made to extend the Drell-Yan cross section measurements to even larger x ($x \lesssim 0.6$) at the J-PARC facility in Japan [35], using a 50 GeV proton beam. The size of the nuclear smearing and nucleon off-shell corrections to the pd/pp cross section ratio is illustrated in Fig. 6 for an average dilepton mass of $Q^2 = 25$ GeV², together with the expected experimental uncertainties. Because of the higher values of x that would be probed here, the effects of the nuclear smearing are expected to be correspondingly more significant than for the lower- x data from the E866

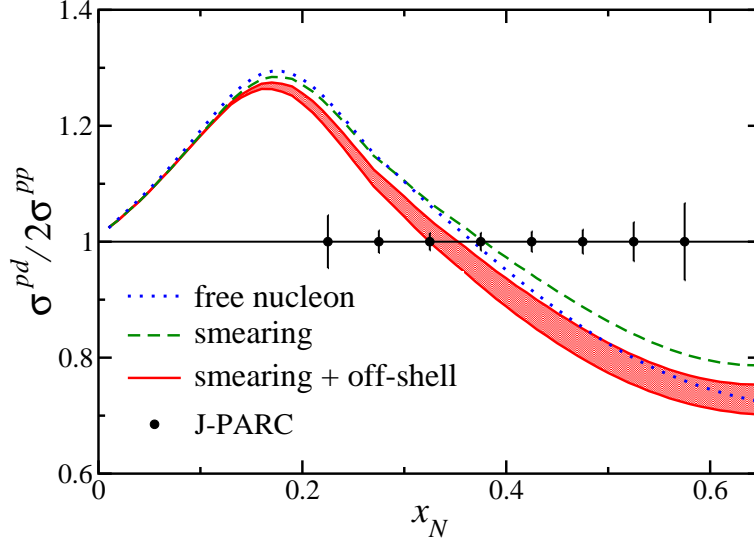


FIG. 6: Ratio of pd to pp Drell-Yan cross sections as in Fig. 4, but at the kinematics of the proposed J-PARC experiment [35], with incident proton energy $k_0 = 50$ GeV and average $Q^2 = 25$ GeV 2 . The projected data (filled circles) with estimated uncertainties are arbitrarily placed at unity.

and SeaQuest experiments, as can be anticipated from Fig. 3. As for the SeaQuest data, the uncertainty range of the nuclear corrections is similar to or larger than the projected experimental uncertainties for $0.25 \lesssim x \lesssim 0.5$, again suggesting the need to better constrain the nuclear corrections if the planned precision is to be reached. Currently, the J-PARC facility is approved for 30 GeV proton running; an upgrade to a 50 GeV proton beam would be needed to realize the goals of the proposed experiment [35, 59].

V. CONCLUSIONS

With the significant improvement in the determination of the \bar{d}/\bar{u} ratio at large values of x expected from upcoming experiments, particularly the SeaQuest Drell-Yan experiment at Fermilab [25], preliminary results from which are anticipated in 2015 [59], the need exists to understand the computation of the cross section with sufficient accuracy for an unambiguous extraction of the signal. In this study we have derived the proton–deuteron dilepton production cross section in terms of the proton–nucleon cross section, paying particular attention to nuclear smearing and nucleon off-shell corrections in the deuteron. The form of the relation between the nuclear and nucleon level cross sections resembles the familiar convolution

result from deep-inelastic scattering [13–16]: in the high energy limit the nucleon light-cone momentum distribution in the deuteron in pd scattering is found to correspond exactly to the Bjorken limit smearing function relevant for describing electron–deuteron scattering in the weak binding approximation [60].

The effects of Fermi motion and nuclear binding contained in the nuclear smearing function are relatively small in the region of x spanned by the existing E866 data, but become more noticeable at the higher x values ($x \gtrsim 0.4$) that will be accessed in the new Fermilab [25] and proposed J-PARC [35] experiments. Corrections arising from the possible off-shell deformation of the nucleon PDFs in the deuteron have been estimated within a simple spectator model of the nucleon that has previously been applied to the analysis of lepton–deuteron deep-inelastic data [14, 19, 20]. For the same range of nucleon swelling parameters as those adopted in the recent CJ global PDF analysis [20], the ratio of pd to pp Drell-Yan cross sections is found to be significantly reduced compared with the free-nucleon calculation. Furthermore, while the nuclear model uncertainty, from both the short-distance part of the deuteron wave function and the nucleon off-shell parameters, is small compared with the existing E866 data, it is of similar size to or even larger than the projected uncertainties for the new SeaQuest experiment in the range $0.15 \lesssim x \lesssim 0.4$. Generally, the magnitude of the corrections and their uncertainties increase with increasing values of x .

These findings suggest that the overall systematic uncertainties in the future measurements may be underestimated at large x , and that further work may be warranted to reduce the theoretical uncertainties on the pd cross section in order to attain the precision goal of the experiments. Although the exact magnitude of the nuclear corrections is subject to some model dependence, the sign of the effect appears universal. In particular, the reduction of the pd cross sections will lead to an increased \bar{d}/\bar{u} ratio extracted from global PDF analyses, with the largest effects expected at the highest x values. While in the present work we have made use of the CTEQ5 parametrization of global PDFs [57] to illustrate the systematics of the nuclear corrections, the results from this analysis will be used in future global QCD fits [61] to obtain a more reliable estimate of the light quark sea distributions in the proton. For future theoretical work, it will also be necessary to reexamine the pion-exchange corrections to pd scattering, which were found in Ref. [24] to be significant at large x . Earlier work on pion-exchange in lepton–deuteron deep-inelastic scattering [26–28] suggested that pion-exchange corrections were important primarily at lower x values, $x \sim 0.1$. A combined

analysis of both nucleonic and pionic contributions within our collinear framework, as well as nuclear shadowing corrections at small x , would then enable a complete description of the nuclear effects in the pd Drell-Yan reaction.

Acknowledgments

We thank D. F. Geesaman, S. Kumano and J.-C. Peng for helpful communications about the proposed Drell-Yan experiments at Fermilab and J-PARC. This work was supported by the DOE Contract No. DE-AC05-06OR23177, under which Jefferson Science Associates, LLC operates Jefferson Lab, and by the NSF and DOD's ASSURE program. The work of A.A. was supported in part by DOE Contract No. de-sc0008791.

-
- [1] P. Amaudruz *et al.*, Phys. Rev. Lett. **66**, 2712 (1991).
 - [2] M. Arneodo *et al.*, Phys. Rev. D **50**, 1 (1994).
 - [3] K. Ackerstaff *et al.*, Phys. Rev. Lett. **81**, 5519 (1998).
 - [4] A. Baldit *et al.*, Phys. Lett. B **332**, 244 (1994).
 - [5] E. A. Hawker *et al.*, Phys. Rev. Lett. **80**, 3715 (1998).
 - [6] R. S. Towell *et al.*, Phys. Rev. D **64**, 052002 (2001).
 - [7] S. Kumano, Phys. Rep. **303**, 183 (1998).
 - [8] J. Speth and A. W. Thomas, Adv. Nucl. Phys. **24**, 83 (1998).
 - [9] G. T. Garvey and J.-C. Peng, Prog. Part. Nuc. Phys. **47**, 203 (2001).
 - [10] J.-C. Peng and J.-W. Qiu, Prog. Part. Nuc. Phys. **76**, 43 (2014).
 - [11] S. D. Drell and T. M. Yan, Phys. Rev. Lett. **25**, 316 (1970).
 - [12] S. D. Ellis and W. J. Stirling, Phys. Lett. B **256**, 258 (1991).
 - [13] S. I. Alekhin, S. A. Kulagin and S. Liuti, Phys. Rev. D **69**, 114009 (2004).
 - [14] S. A. Kulagin and R. Petti, Nucl. Phys. **A765**, 126 (2006).
 - [15] Y. Kahn, W. Melnitchouk and S. Kulagin, Phys. Rev. C **79**, 035205 (2009).
 - [16] A. Accardi, J. W. Qiu, and J. P. Vary, "Collinear factorization and deep inelastic scattering on nuclear targets" (2011, unpublished).
 - [17] S. Alekhin, J. Blümlein, S. Klein and S.-O. Moch, Phys. Rev. D **81**, 014032 (2010).

- [18] A. Accardi, M. E. Christy, C. E. Keppel, P. Monaghan, W. Melnitchouk, J. G. Morfin and J. F. Owens, Phys. Rev. D **81**, 034016 (2010).
- [19] A. Accardi, W. Melnitchouk, J. F. Owens, M. E. Christy, C. E. Keppel, L. Zhu, and J. G. Morfin, Phys. Rev. D **84**, 014008 (2011).
- [20] J. F. Owens, A. Accardi and W. Melnitchouk, Phys. Rev. D **87**, 094012 (2013).
- [21] L. T. Brady, A. Accardi, W. Melnitchouk and J. F. Owens, JHEP **1206**, 019 (2012).
- [22] P. Jimenez-Delgado, W. Melnitchouk and J. F. Owens, J. Phys. G: Nucl. Part. Phys. **40**, 093102 (2013).
- [23] W. Melnitchouk, J. Speth and A. W. Thomas, Phys. Rev. D **59**, 014033 (1998).
- [24] H. Kamano and T. -S. H. Lee, Phys. Rev. D **86**, 094037 (2012).
- [25] Fermilab E906 experiment (SeaQuest), *Drell-Yan Measurements of Nucleon and Nuclear Structure with the Fermilab Main Injector*, D. F. Geesaman and P. E. Reimer, spokespersons; <http://www.phy.anl.gov/mep/SeaQuest/index.html>.
- [26] L. P. Kaptari and A. Yu. Umnikov, Phys. Lett. B **272**, 359 (1991).
- [27] W. Melnitchouk and A. W. Thomas, Phys. Rev. D **47**, 3783 (1993).
- [28] N. N. Nikolaev and W. Schafer, Phys. Lett. B **398**, 245 (1997), [Erratum-ibid. B **407**, 453 (1997)].
- [29] F. Gross and S. Liuti, Phys. Rev. C **45**, 1374 (1992).
- [30] C. Ciofi degli Atti, D. B. Day and S. Liuti, Phys. Rev. C **46**, 1045 (1992).
- [31] W. Melnitchouk, A. W. Schreiber and A. W. Thomas, Phys. Rev. D **49**, 1183 (1994).
- [32] W. Melnitchouk, A. W. Schreiber and A. W. Thomas, Phys. Lett. B **335**, 11 (1994).
- [33] S. A. Kulagin, G. Piller and W. Weise, Phys. Rev. C **50**, 1154 (1994).
- [34] W. Cosyn, W. Melnitchouk and M. Sargsian, Phys. Rev. C **89**, 014612 (2014).
- [35] J-PARC proposal P04, *Measurement of high-mass dimuon production at the 50-GeV proton synchrotron*, J.-C. Peng and S. Sawada spokespersons; <http://j-parc.jp/index-e.html>.
- [36] S. Kumano, J. Phys. Conf. Ser. **312**, 032005 (2011).
- [37] P. J. Mulders, “*Transverse momentum dependence in structure functions in hard scattering processes*”, lecture notes, <http://www.nikhef.nl/~pietm/COR-0.pdf>, 2001 (unpublished).
- [38] S. A. Kulagin, W. Melnitchouk, G. Piller and W. Weise, Phys. Rev. C **52**, 932 (1995).
- [39] S. A. Kulagin and W. Melnitchouk, Phys. Rev. C **78**, 065203 (2008).
- [40] M. Lacombe *et al.*, Phys. Lett. B **101**, 139 (1981).

- [41] R. B. Wiringa, V. G. J. Stoks and R. Schiavilla, Phys. Rev. C **51**, 38 (1995).
- [42] R. Machleidt, Phys. Rev. C **63**, 024001 (2001).
- [43] F. Gross and A. Stadler, Phys. Rev. C **78**, 014005 (2008).
- [44] L. Frankfurt and M. Strikman, Phys. Lett. **76** B, 333 (1978); Phys. Rep. **76**, 215 (1981).
- [45] J. J. Ethier, N. Doshi, S. Malace and W. Melnitchouk, Phys. Rev. C **89**, 065203 (2014).
- [46] R. K. Ellis, W. Furmanski and R. Petronzio, Nucl. Phys. **B212**, 29 (1983).
- [47] J. W. Qiu, Phys. Rev. D **42**, 30 (1990).
- [48] A. Accardi and J. W. Qiu, JHEP **0807**, 090 (2008).
- [49] W. Melnitchouk, M. Sargsian and M. I. Strikman, Z. Phys. A **359**, 99 (1997).
- [50] F. E. Close, R. L. Jaffe, R. G. Roberts and G. G. Ross, Phys. Rev. D **31**, 1004 (1985).
- [51] J. J. Ethier and W. Melnitchouk, Phys. Rev. C **88**, 054001 (2013).
- [52] M. Glück, E. Reya and A. Vogt, Eur. Phys. J. C **5**, 461 (1998).
- [53] P. Jimenez-Delgado and E. Reya, Phys. Rev. D **79**, 074023 (2009).
- [54] P. Jimenez-Delgado and E. Reya, Phys. Rev. D **89**, 074049 (2014).
- [55] D. M. Alde *et al.*, Phys. Rev. Lett. **64**, 2479 (1990).
- [56] P. L. McGaughey *et al.*, Phys. Rev. Lett. **69**, 1726 (1992).
- [57] H. L. Lai *et al.*, Eur. Phys. J. C **12**, 375 (2000).
- [58] J. C. Collins, D. E. Soper and G. F. Sterman, Adv. Ser. Direct. High Energy Phys. **5**, 1 (1988).
- [59] J.-C. Peng and D. F. Geesaman, private communication.
- [60] W. Melnitchouk, AIP Conf. Proc. **1261**, 85 (2010).
- [61] J. F. Owens *et al.*, in preparation.